M. SATERNUS*,#, T. MERDER*, J. PIEPRZYCA*

THE INFLUENCE OF IMPELLER GEOMETRY ON THE GAS BUBBLES DISPERSION IN URO-200 REACTOR – RTD CURVES

WPŁYW RODZAJU WIRNIKA NA DYSPERSJĘ PĘCHERZYKÓW GAZOWYCH W REAKTORZE URO-200 – KRZYWE MIESZANIA

URO-200 reactor belongs to batch reactors used in refining process of aluminium and its alloys in polish foundries. The appropriate level of hydrogen removal from liquid aluminium can be obtained when the mixing of inert gas bubbles with liquid metal is uniform. Thus, the important role is played by the following parameters: flow rate of refining gas, geometry of the impeller, rotary impeller speed.

The article presents the results of research conducted on physical model of URO-200 reactor. The NaCl tracer was introduced to water (modelling liquid aluminium) and then the conductivity was measured. Basing on the obtained results the Residence Time Distribution (RTD) curves were determined. The measurements were carried out for two different rotary impellers, flow rate equaled 5, 10, 15 and 20 dm^3/min and rotary impeller speed from 250 to 400 rpm every 50 rpm.

Keywords: aluminium refining, gas dispersion, physical modelling, RTD-curves.

Rektor URO-200 jest reaktorem cyklicznym stosowanym powszechnie w Polsce do procesu rafinacji aluminium i jego stopów. Odpowiedni stopień usuwania wodoru z ciekłego aluminium uzyskuje się wówczas, gdy wymieszanie ciekłego metalu z pęcherzykami gazu obojętnego jest równomierne. Ważną rolę odgrywają takie parametry procesowe jak: natężenie przepływu gazu, kształt wirnika oraz prędkość obrotowa rotora.

W artykule przedstawiono wyniki badań w oparciu o model fizyczny reaktora URO-200. Mierzono konduktywność roztworu wodnego (modelującego ciekłe aluminium), do którego wprowadzano znacznik NaCl. W oparciu o otrzymane wyniki wykreślono krzywe mieszania RTD (Residence Time Distribution). Pomiary prowadzono dla dwóch różnych wirników przy natężeniu przepływu gazu 5, 10, 15 i 20 dm^3/min oraz przy obrotach wirnika 250, 300, 350 i 400 obr/min.

1. Introduction

Nowadays, aluminium is the second metal taking into account the production. It can be obtained from ores electrolitically (primary aluminium – 2/3 of the total production) or from scrap by melting (secondary aluminium – 1/3 of the total production). However, independently of the production methods all aluminium should be refined. The main reason is to remove the harmful hydrogen which, when the level is higher than 0.1 ppm, can cause the porosity and as a consequence the aluminium quality is decreased [1,2]. Additionally, refining process also gives possibility to remove by flotation other undesirable impurities such as: oxides, borides, carbides [3,4].

There are many physical and chemical methods of refining, however nowadays barbotage has become the most popular that means introduction of many inert gas bubbles into the reactor using of ladle, rotary impeller or ceramic porous plugs. The gas bubbles capture the hydrogen and pick it up to the surface. It is really important to obtain uniform dispersion of gas bubbles in the whole volume of the liquid metal. The way of gas introduction plays significant role in getting such dispersion level; after all, the processing parameters like rotary impeller speed or flow rate of refining gas are very important.

Many refining reactors are used all over the world [5-15], e.g. DUFI, Alcoa 622, DMC, MINT, SNIF, GBF, RDU, ACD), but in Poland the most popular is URO-200 reactor. Such reactor is easy to operate and can work in a crucible or directly in a furnace. It is a bath reactor (designed in IMN-OML Skawina) using rotary impeller to introduce the refining gas into the metal. However, if such reactor works properly, the processing parameters (such as flow rate of gas and rotary impeller speed) can be chosen appropriately. For this purpose the most adequate is to use modelling methods. This kind of a research is applied commonly in processes of steel and nonferrous metals metallurgy [16-24] to get information about hydrodynamic phenomena occurring in liquid metal. Mainly physical modelling is rather cheap (water is used as a modelling agent) and not complicated comparing to carrying out experimental research in industry. Not to mention, that in some cases such tests in industrial conditions are even not possible to conduct.

* SILESIAN UNIVERSITY OF TECHNOLOGY, INSTITUTE OF METALS TECHNOLOGY, 8 KRASINSKIEGO STR, 40-019 KATOWICE, POLAND

Corresponding author: mariola.saternus@polsl.pl

2888

2. Experimental procedure

Fig. 1 presents the water model of URO-200 reactor. It was built in the 1:1 scale. According to the theory of similarity in modelling research of hydrodynamic and isothermal flows, taking into consideration the thermal and chemical effect is not necessary. Thus, the similarity of the model to the URO-200 reactor was realized considering the geometric, dynamic and kinetic similarity. To determine the dynamic similarity, the rule of criterial numbers equality in the model and the real reactor was applied. Whereas, the kinetic similarity was determined by means of the scales method using modified Froude`s number. Table 1 shows the values of the most important criterial numbers such as Reynolds, Froude and Weber number, calculated for water at the temperature 293 K and aluminium at the temperature 973 K.
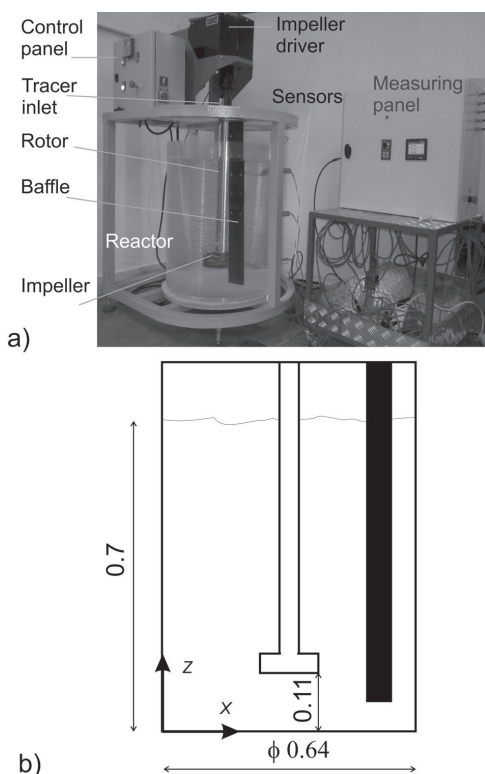
TABLE 1

Calculated values of criterial numbers for water and aluminium in the URO-200 reactor

Values for:	Reynolds number	Froude number	Weber number
Water at 293 K	27802	84.24	0.0029
Aluminium at 973 K	67392	21.41	0.0029

The research was carried out for two different rotary impellers varying the geometry and the way of introducing the refining gas into the fluid. Fig. 2a shows such impellers with the marked main dimensions (impeller diameter, the height of the impeller and in case of impeller A also the diameter of the hole, through which the gas bubble is introduced into the metal). In the impeller A the refining gas bubbles are introduced into the metal through eight holes 1 mm (diameter) which are symmetrically placed at the impeller perimeter. While in the case of impeller B, the refining gas is introduced by the system of channels placed in the geometry of impeller.

The research was carried out using test stand presented in Fig. 2b, and was divided into two stages. The first stage includes visualization experiments. When the media flow was stabilized according to the determined similarity conditions, the registration began by means of digital camera. Such measurements allow to estimate the influence of refining gas flow on the level of refining gas dispersion in the water. The second stage includes the measurements of the conductivity of modelling liquid in the reactor, which is the response to the signal input function (Dirac`s impulse) by the action of tracer (NaCl). When the media flow was stabilized according to the determined similarity conditions, tracer (small amount of the water solution of NaCl) was introduced to the system for 5s. The changes of tracer concentration, represented by the changes of modelling liquid conductivity, were registered continuously using three conductometers. Fig. 2b shows the places of tracer introduction and the location and designation of conductivity sensors.

During experimental tests the flow rate of refining gas was changing from 5 to 20 dm^3/min; whereas the rotary impeller speed from 250 to 400 rpm every 50 rpm. Table 2 presents the processing parameters used in the research.

Fig. 1. The water model of the URO-200 reactor: a) view and the main elements, b) main dimensions (in m)
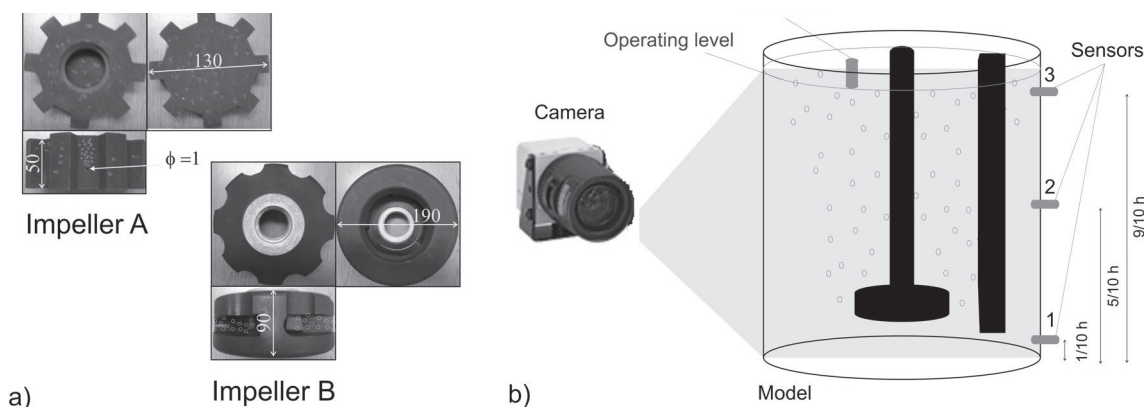

Fig. 2. a) The impellers analyzed in the research with their dimensions, b) scheme of the test stand used in the modelling research

TABLE 2

Processing parameters and designation of the experiments

Case A (Impeller A)	A1	A2	A3	A4	A5	A6	A7	A8	A9	A10	A11	A12	A13	A14	A15	A16
Case B (Impeller B)	B1	B2	B3	B4	B5	B6	B7	B8	B9	B10	B11	B12	B13	B14	B15	B16
Rotary impeller speed [rpm]	250				300				350				400			
Flow rate of refining gas [dm³/min]	5	10	15	20	5	10	15	20	5	10	15	20	5	10	15	20

3. Results and discussion

The construction of the impeller influences greatly the shape and amount of generated gas bubbles. Fig. 3 shows the gas bubbles generated by two different impellers without rotation (Fig. 3a and b – 0 rpm), and when the rotary impeller speed was 250 and 350 rpm. Such pictures show how the gas bubbles are generated by those impellers.

Generally six different shapes of gas bubbles can be distinguished: spherical, ellipsoidal, dimpled ellipsoidal cap, skirted, spherical cap and wobbling [25]. The best is the one where spherical small gas bubbles are created (to obtain good level of gas dispersion). Refining gas in case of impeller A is introduced into the metal through holes with small diameter. There are many gas bubbles, which are not spherical, irregular and big; going up to the surface near the impeller shaft. Refining gas in case of impeller B is introduced into the metal through system of channels placed in the geometry of the impeller. The gas bubbles are rather spherical; but they are only a few bubbles, but very big ones. So the dispersion of the gas bubbles in the metal in such case is almost impossible.

When there is rotation (in both cases), even at the minimal level (250 rpm); the generated gas bubbles are considerably smaller, which really improve the dispersion level in the whole reactor. Fig. 4 and 5 presents the level of gas dispersion in the modelling liquid for the analyzed cases. Generally the dispersion level of gas bubbles in the metal can be divided into four types: minimal dispersion, intimate dispersion, uniform dispersion and the case when swirls and chain flow are observed. The last one is unfavourable, because it can cause that the hydrogen is again picked up from the surface. The most desirable is uniform dispersion, in that case the gas bubbles are observed in the whole reactor, even below the rotary impeller. Comparing both rotary impellers (A and B) it was seen that in the small rotary speed impeller (lower than 250 rpm) the minimal dispersion was observed. When the rotary impeller was 250 rpm to 300 rpm the intimate dispersion was seen, in case of impeller B even at 350 rpm. The uniform dispersion was observed when the rotary impeller speed was between 350 to 400 rpm and the flow rate from 10 to 15 dm³/min.
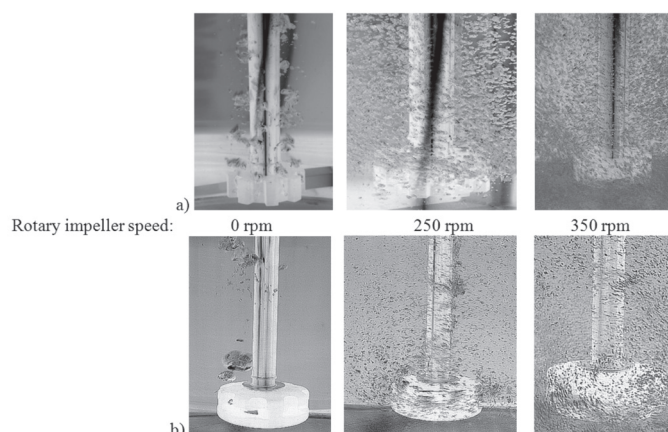

Fig. 3. View of gas bubbles generated by rotary impeller: a) A-type, b) B-type; flow rate of refining gas equals 10 dm³/min

Fig. 6 presents the dimensionless characteristics of mixing for the particular sensors. To obtain dimensionless concentration of the tracer (in order to compare the results of conducted experiment objectively in all variants) the following equations were used:

$$C = C_{exp}/C_{max} \qquad (1)$$

$$C_b = C - C_0/C_\infty - C_0 \qquad (2)$$

where: C_{exp} – tracer concentration in time, C_b – dimensionless tracer concentration, C_0 – initial tracer concentration, C_{max} – maximum tracer concentration, C_∞ - final tracer concentration.

Considering curves presented in Fig. 6, it was stated that there are substantial differences between these curves for the particular sensors. When analyzing these curves it can be seen that at the same processing parameters different condition of mixing in the reactor can be created. In the case, when the time of tracer reaching the sensor was the shortest then the parameters did not allow to obtain uniform mixing of the gas bubbles with the liquid in the whole volume of the reactor. When this time was relatively long, then it reached the conditions which allowed to uniform mixing of gas bubbles in the whole reactor.
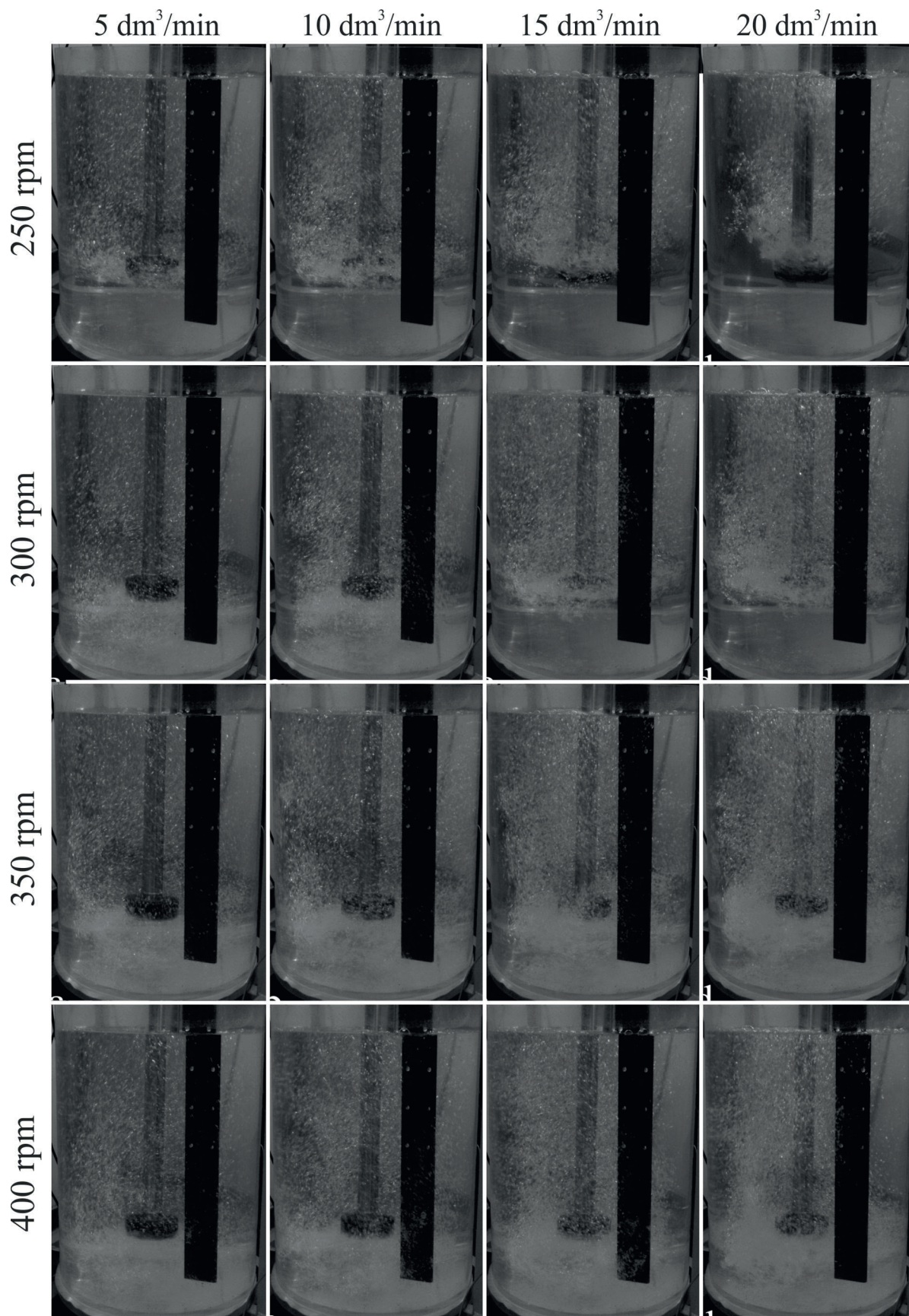
Fig. 4. Results of visualization research conducted for the water model of URO-200 reactor for the impeller A
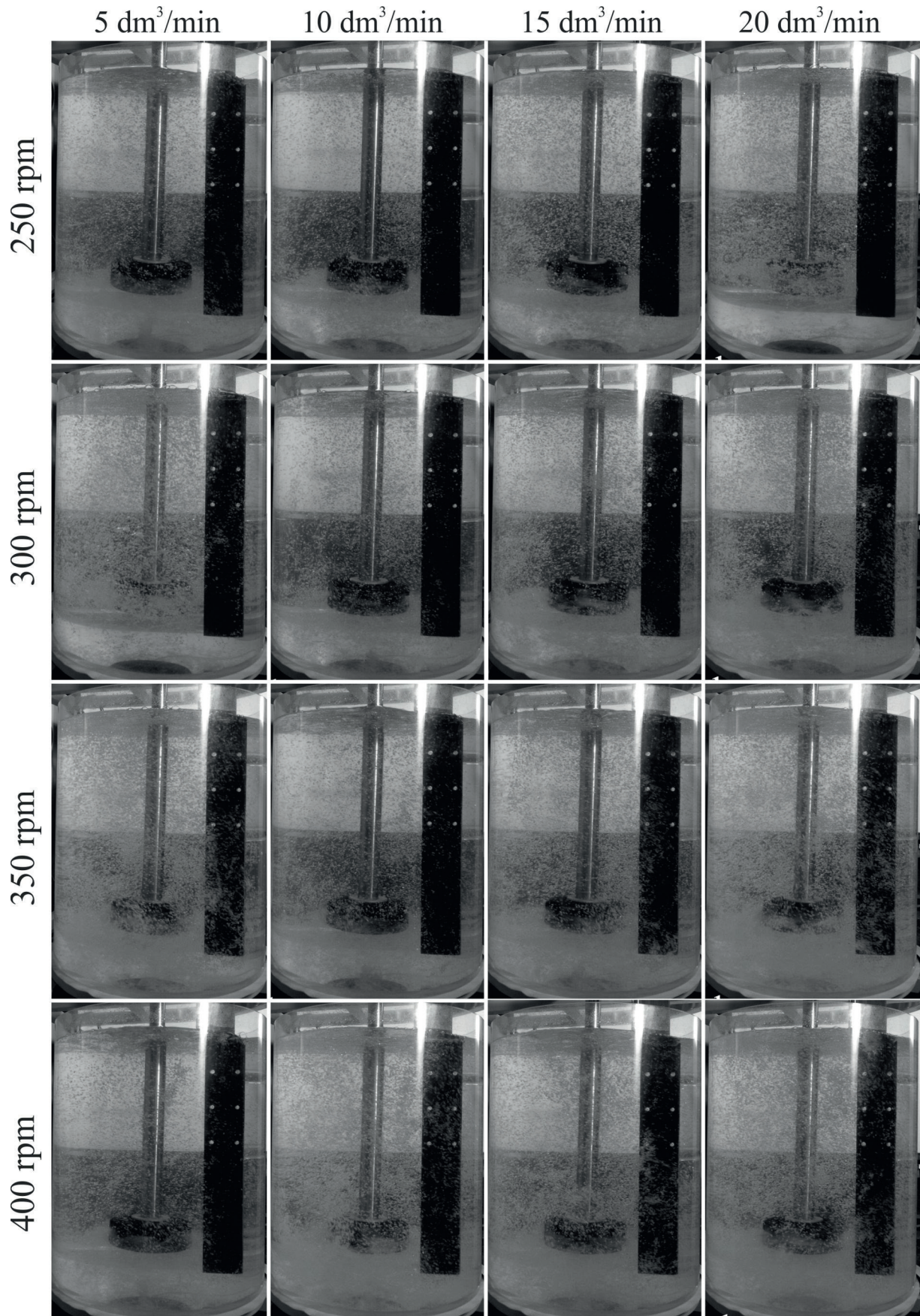
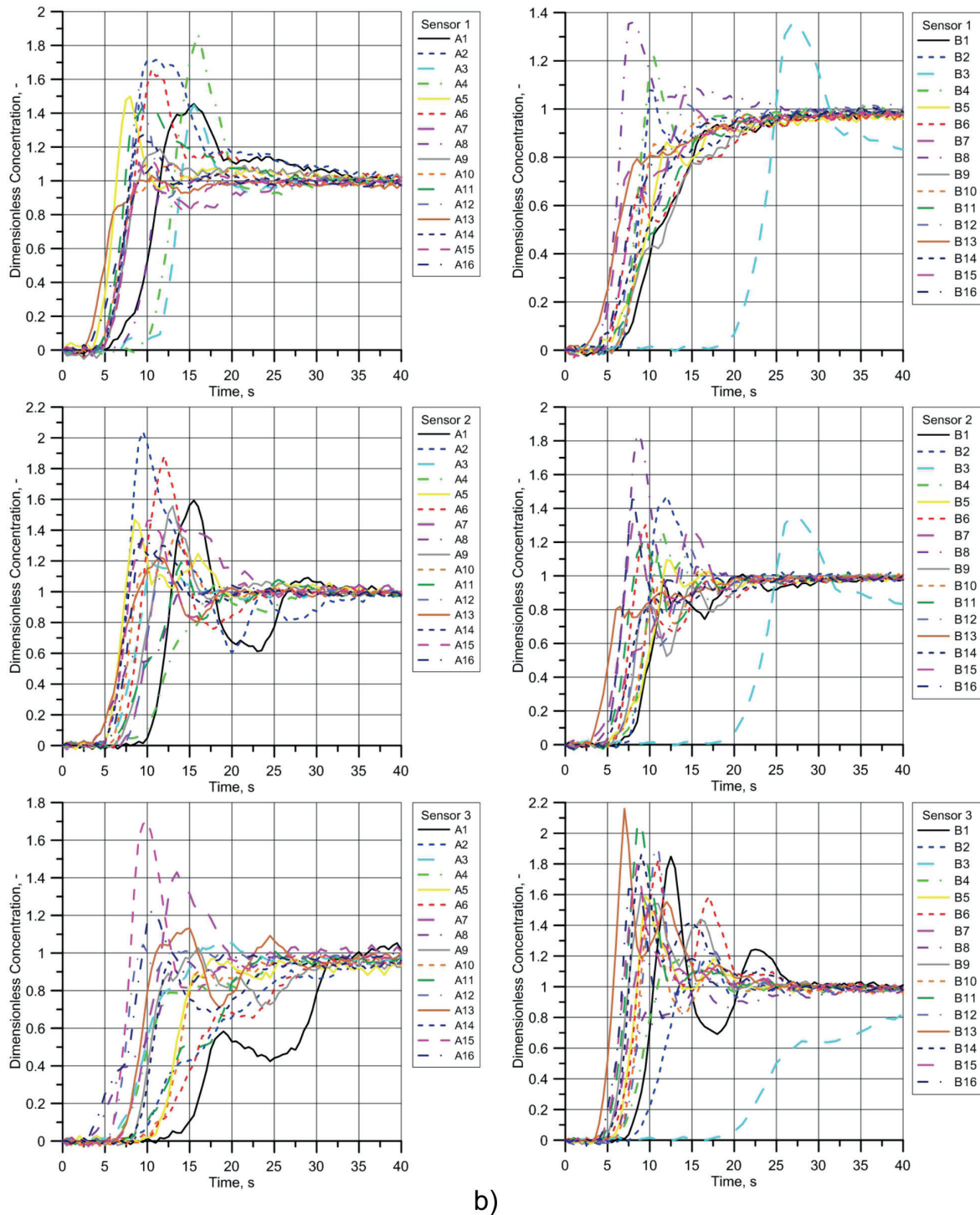Fig. 5. Results of visualization research conducted for the water model of URO-200 reactor for impeller B

Fig. 6. Dimensionless characteristics of mixing for three different sensors for: a) impeller A, b) impeller B

Physical modelling does not give full information about the flow of liquid and gas; numerical simulations would complement and broaden the results coming from the physical modelling concerning such information like the velocity field distribution, turbulence distribution or even the participation of the gaseous phase in the analyzed object. Thus, the next stage of the research should be numerical calculation for the studied impellers. Now, it can be stated that the chosen impellers need comparable processing parameters.

4. Summary and conclusions

Applying the techniques of physical modelling becomes an effective way of replacing the difficult and expensive experimental research conducted in industry; in the same time giving information about the optimal parameters of the process. The obtained results can be valuable also considering the qualitative (dispersion of gas bubbles in the liquids) and quantitative (mixing curves) verification of the results coming from the numerical modelling.

The experimental research carried out on the water model of URO-200 reactor enabled to work out the characteristics of mixing and determine the kind of refining gas dispersion in the reactor using two different rotary impellers. The analysis of such characteristics allows to present the following conclusions:

- In order to obtain uniform dispersion in the whole volume of the reactor, processing parameter such as rotary impeller speed and flow rate of refining gas should be precisely determined according to the geometry of the applied impeller.
- For both kinds of examined impellers some disturbances at the free surface were observed when the highest rotary impeller speed and also flow rate of refining gas were tested - this as a consequence can lead to the situation when hydrogen is again absorbed by the liquid metal.
- Optimal processing parameters for impeller A are the following: rotary impeller speed 350 rpm and flow rate of refining gas 15 dm^3/min; whereas for the impeller B: rotary impeller speed 400 rpm and flow rate of refining gas 10 dm^3/min – in that cases the time of tracer coming to the sensor is relatively long, thus the determined characteristics of mixing confirmed the results obtained from visualization research.

REFERENCES

[1] M. Saternus, Metalurgija **50** (4), 257-260 (2011).

[2] M.B. Taylor, Aluminium **79** (1-2), 44-50 (2003).

[3] J.Y. Oldshue, Fluid Mixing Technology, Chemical engineering, McGraw-Hill Publications Co., New York 1983.

[4] K. Onopiak., J. Botor, Archives of Metallurgy and Materials **51** (3), 443-450 (2006).

[5] M. Saternus, J. Botor, Metalurgija **48** (3), 175-179 (2009).

[6] J.M. Chateau, Aluminium Times **04/05**, 34-35 (2003).

[7] D.C. Chesonis, D.H. De Young, E. Elder, R.O. Wood, Light Metals, TMS, 745-750 (2000).

[8] S. Kato, Sumitomo Light Metal Techncial Report 34(3), 59-77 (1993).

[9] Z. L ifeng, L. Xuewei, T.A. Tryg, M. Long, Mineral Processing and Extractive Metallurgy Review **32** (3), 150-228 (2011).

[10] T. Kumaresan, J.B. Joshi, Chemical Engineering and Processing **115** (3) 173-193 (2006).

[11] G. Maeland, E. Myrbostad, K. Venus, Light Metals, TMS, 855-859 (2002).

[12] E. Waz, J. Carre, P. Le Brun, A. Jardy, C. Xuereb, D. Ablitzer, Light metals, TMS, 901-907 (2003).

[13] K.A. Carpenter, M.J. Hanagan, Light metals, TMS, 1017-1020 (2001).

[14] P. Le Brun, Light Metals, TMS, 869-875, (2002).

[15] P.J. Flisakowski, J.M. McCollum, R.A. Frank, Light Metals, TMS, 1041-1047 (2001).

[16] B. Panic, Metalurgija **52** (2), 177-180 (2013).

[17] M. Tkadleckova, P. Machovcak, K. Gryc, K. Michalek, L. Socha, P. Klus, Archives of Metallurgy and Materials **58**, 1, 171-177 (2013).

[18] M. Warzecha, J. Jowsa, T. Merder, Metalurgija **46** (4), 227-232 (2007).

[19] A. Fornalczyk, S. Golak, R. Przyłucki, Archives of Civil and Mechanical Engineering **15** (1), 171-178 (2015).

[20] M. Saternus, T. Merder, P. Warzecha, Solid State Phenomena **176**, 1-10 (2011).

[21] T. Merder, J. Pieprzyca, Steel Research International **11**, 1029-1038 (2012).

[22] B. Panic, K. Janiszewski, Metalurgija **53** (3), 331-334 (2014).

[23] J. Barglik, A. S malcerz, R. Dolezel, Journal of Computational and Applied Mathematics **270**, 231-240 (2014).

[24] J.L. Camacho–Martinez, M.A. Ramirez–Argaez, A. Juarez–Hernandez, C. Gonzalez–R ivera, G. Trapaga–Martinez, Materials and Manufacturing Processes **27**, 556-560 (2012).

[25] R. Lift, J.R. Grace, M.E Weber, Bubbles, drops and particles, Academic Press, New York 1978.